

Fig. E-1
 Contact stress distributions computed in the finite element analysis are shown at a series of stages over an entire duty cycle of simulated ankle motion, for the intact, defect (no implant), baseline, proud, and recessed implantation states.

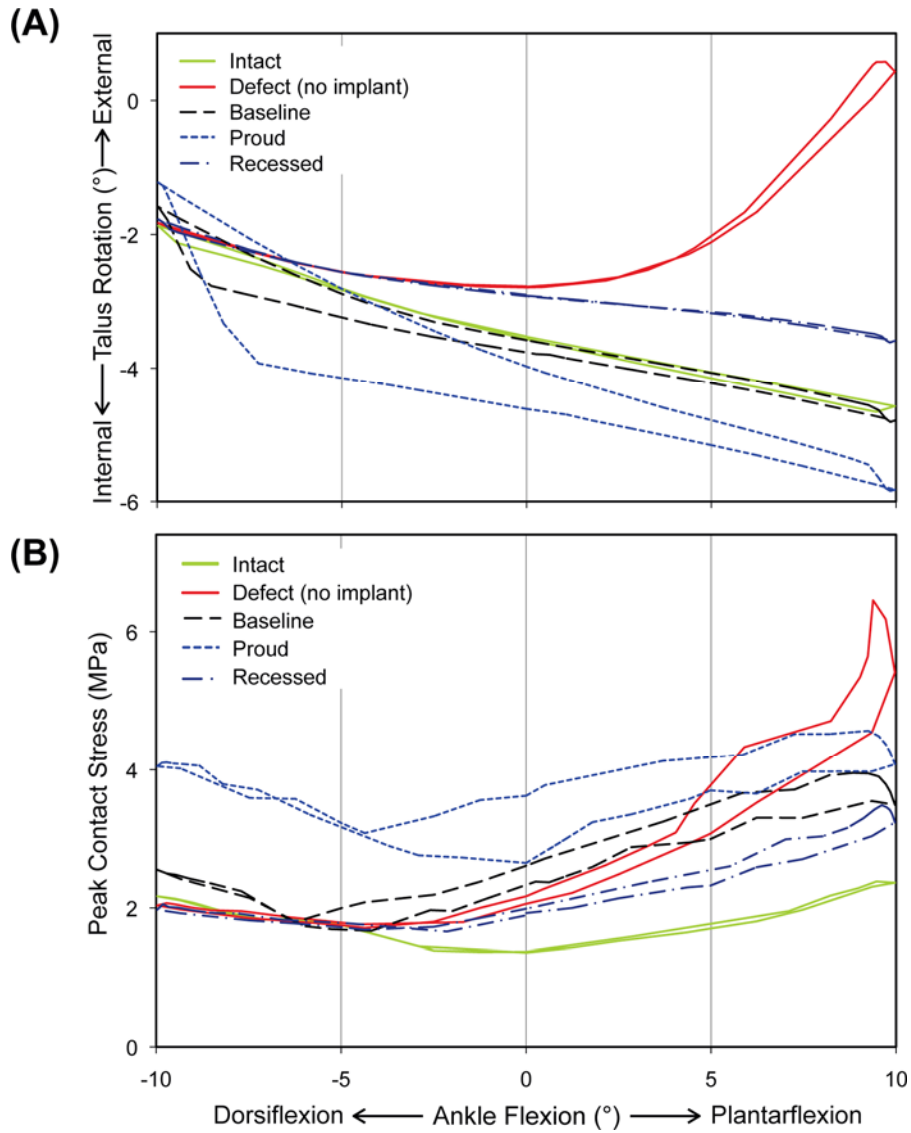


Fig. E-2

Talar kinematics (A) and peak contact stress (B) computed in the finite element analysis are plotted across a range of ankle flexion for the intact, defect (no implant), baseline, proud, and recessed implantation states.

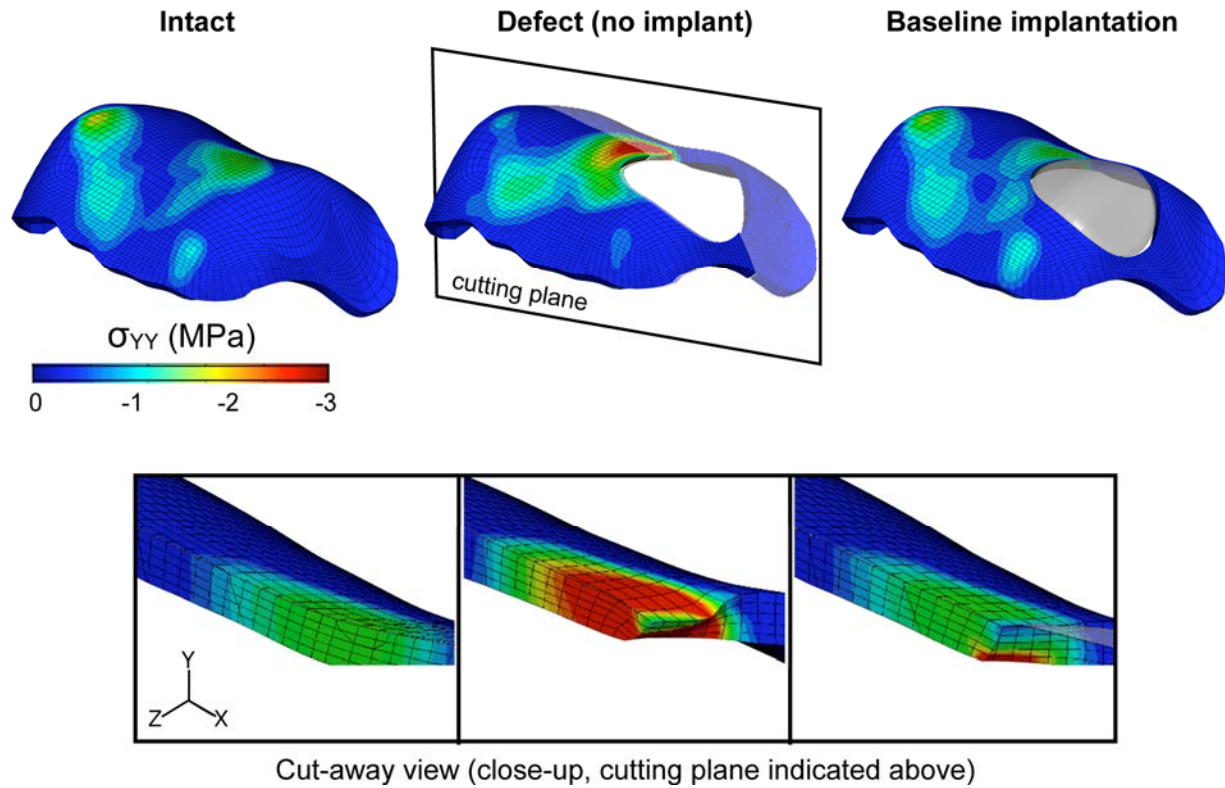


Fig. E-3

Axial cartilage stress (σ) contours computed in the finite element analysis are shown at terminal (10°) plantar flexion for the intact, defect (no implant), and baseline implantation states. Note that values are negative, indicating compressive stress.

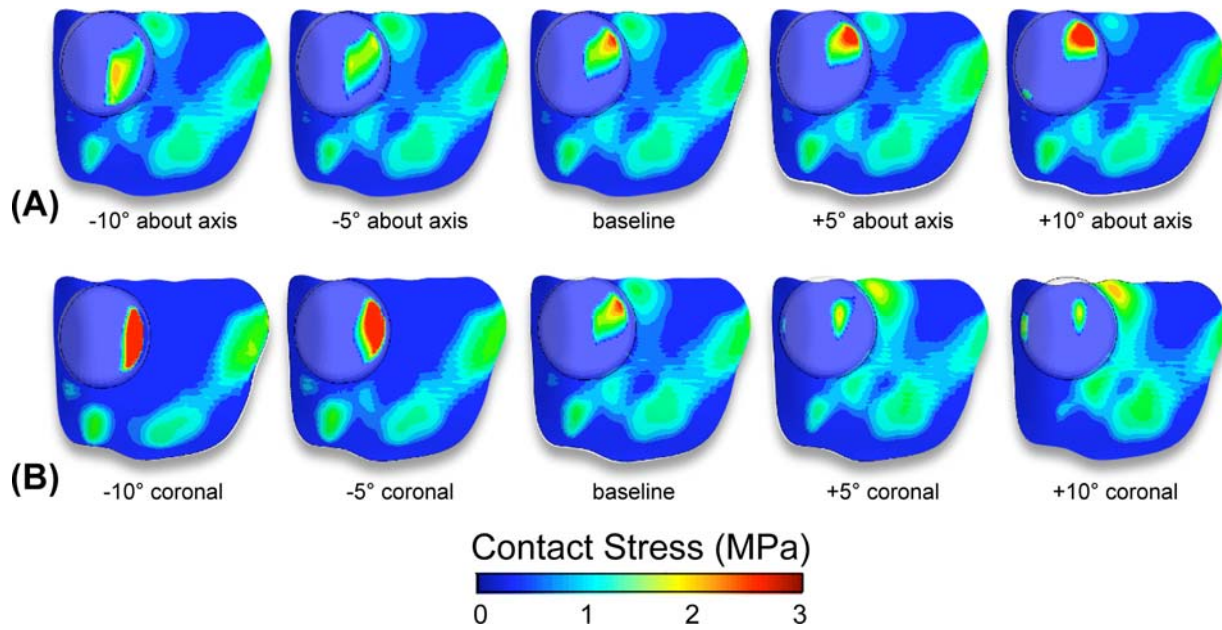


Fig. E-4

Contact stress contours computed in the finite element analysis, showing the variations associated with implantation of the cap at various angles about the implant post axis (A) and coronally rotated about the medial edge of the talus (B), for the case of 5° of ankle plantar flexion.